


Article

Environmental Performance of Innovative Ground-Source Heat Pumps with PCM Energy Storage

Emanuele Bonamente ^{1,2,*}  and Andrea Aquino ³¹ Department of Engineering, University of Perugia, 06125 Perugia, Italy² CIRIAF—Interuniversity Research Center on Pollution and Environment, University of Perugia, 06125 Perugia, Italy³ Department of Mechanical and Industrial Engineering, University of Brescia, 25123 Brescia, Italy; andrea.aquino@unibs.it

* Correspondence: emanuele.bonamente@unipg.it

Received: 19 November 2019; Accepted: 23 December 2019; Published: 25 December 2019



Abstract: Space conditioning is responsible for the majority of carbon dioxide emission and fossil fuel consumption during a building's life cycle. The exploitation of renewable energy sources, together with efficiency enhancement, is the most promising solution. An innovative layout for ground-source heat pumps, featuring upstream thermal energy storage (uTES), was already proposed and proved to be as effective as conventional systems while requiring lower impact geothermal installations thanks to its ability to decouple ground and heat-pump energy fluxes. This work presents further improvements to the layout, obtained using more compact and efficient thermal energy storage containing phase-change materials (PCMs). The switch from sensible- to latent-heat storage has the twofold benefit of dramatically reducing the volume of storage (by a factor of approximately 10) and increasing the coefficient of performance of the heat pump. During the daily cycle, the PCMs are continuously melted/solidified, however, the average storage temperature remains approximately constant, allowing the heat pump to operate closer to its maximum efficiency. A life cycle assessment (LCA) was performed to study the environmental benefits of introducing PCM-uTES during the entire life cycle of the system in a comparative approach.

Keywords: ground-source heat pumps; space conditioning; environmental sustainability; life cycle assessment (LCA); phase-change material (PCM)

1. Introduction

Buildings dramatically contribute to worldwide energy use and greenhouse gas (GHG) emissions. According to last official European Union reports [1,2], in 2010 the building sector accounted for about 32% of worldwide final energy consumption and 34% of global GHG emissions. More recently, the Intergovernmental Panel on Climate Change (IPCC) updates confirmed the energy share (31%, [3]) and reduced the estimates of greenhouse gas emissions (23%, [4]). However, both values are expected to increase, resulting in further energy consumption (+2 billion tons of oil equivalent [5]) for the construction of new living spaces worldwide (+230 billion square meters), causing an estimated +30% increase in GHG emissions in the next 40 years. In this context, government and international organizations are pursuing new and more severe policies specifically aimed at reducing the energy consumption of the building sector and mitigating associated emissions. As an example, the European Union aims to reduce by 90% the equivalent carbon dioxide (CO₂e) emissions of buildings by the year 2050, estimating that about the 17% of the primary energy saving is achievable by retrofitting existing

buildings. The potential energy savings of an existing building are strictly related to its heating and cooling systems. During the entire building's life cycle (from construction to demolition), a major share of the required energy (80–90%) is associated with operating energy [6], and up to 60% of the total energy consumption is due to air-conditioning [7]. The enhancement of air-conditioning energy efficiency, coupled with an integration of renewable-energy technologies, is considered an effective solution to mitigate the environmental impacts of buildings [8–12].

Among the renewable energy systems for space conditioning [13], ground-source heat pumps (GSHPs) have a wide diffusion rate because of their low operative temperature. Low-temperature heat sources (soil or underground water) between 5 and 30 °C are found easily worldwide as they are available at reasonable depths [14,15]. GSHPs exchange heat with the first layer of the ground via properly designed borehole heat exchangers (BHEs) and, due to the low operative temperatures of the working cycle, their feasibility does not depend on the nature of the geothermal resources available at the building site [16]. Like conventional heat pump (HP) systems, GSHPs need electricity as the driving energy in order to transfer heat from a cold source to a hot source. During the heating season, the heat is extracted from the ground and given to the indoor space. Meanwhile, during the cooling season the cycle is reversed. The coefficient of performance (COP), defined as the ratio of total output energy (i.e., heat transfer to/from the building) to the total power input, measures the overall system efficiency. This is the only indicator recognized by technical regulations [17] to evaluate the environmental performance of an HP system, which is classified as a renewable energy system only if the measured COP exceeds a minimum value (3.2 to 3.5 for typical geothermal applications [18]). However, the exploitation of geothermal resources is affected by several environmental implications and a comprehensive environmental impact assessment of a GSHP cannot be limited to its energy performance. Additional negative environmental impacts should be considered, such as the risks of aquifer contamination or the contribution to soil compaction and habitat loss or disturbance. An important source of such impacts is the excavation of BHEs, which can also affect initial costs by up to 50% of the total investment [19].

Thermal energy storage (TES) is a key component of the optimization of the performance of a building energy system and the reduction of its environmental impact [20,21]. Thermal energy can be stored in three main forms: sensible heat, latent heat, and thermo-chemical energy. Sensible storage devices commonly use water as a storage material because of its well-known properties, availability, and negligible cost. However, these systems require important storage volumes with relatively high costs. Latent heat TES makes use of the enthalpy change of a material during its phase transition in order to provide higher energy density than sensible systems. As a consequence, latent heat systems need smaller storage volumes than sensible ones. Conventional materials (e.g., water, diathermic oil, etc.) change phase at temperatures that are not optimal for air-conditioning applications. On the other hand, phase change materials (PCMs) make the latent heat storage available at a large range of operative temperatures, including those favorable for indoor air-conditioning. These materials are easily suited to several heating and cooling applications due to the wide market offer in terms of thermal properties and packaging: PCMs are commonly available both in packaged volumes, as spheres, panels, etc. (i.e., encapsulated PCMs), or without packaging (i.e., free-form PCMs) [22,23].

Previous studies on GSHP systems [24,25] have shown that final COP depends on system configuration and local site conditions (e.g., the BHEs setup, the climate, the ground properties, and the HP nominal power), as well as the transient operative conditions of the system's duty-cycle: the ground's undisturbed temperature, the temperature difference between the surface and the underground, and the temperature of the water leaving the heat pump and the BHEs. These temperature fluctuations lower the system COP. The performance of GSHP gradually decays with operating time because of the continuous injection of heat into the ground (cooling cycle), which increases its undisturbed temperature [26]. The heating cycle produces a similar effect that presents as an inverted temperature trend [27]. A general explanation of this issue is that gradual COP reduction is due to an unbalanced (over the yearly season) heat exchange between the system and the ground [28]. The effects of this

thermal imbalance by a two-year on-site measurement campaign were a decrease in system COP by 42% and 26% in the winter and summer season, respectively [29].

The role of a TES is essentially to decouple the thermal energy exchange of the ground from the building demand by accumulating thermal energy (heat or cold) when it is more readily available and using it upon request. This mismatch could attenuate the effects derived from temperature fluctuations in system efficiency and, therefore, several works aim to include a TES system in the standard GSHP layout. The two approaches can be identified as:

1. Enhancement of the thermal capacity of the system by upgrading a specific component (BHEs or air distribution system);
2. Direct installation of a TES.

The first approach is illustrated in [30]. A laboratory-scale BHE with PCM included in its backfill was tested. The system successfully delayed the ground temperature variation and reduced the thermal interference radius (i.e., less area was required for installation). Furthermore, the constant temperature of phase change improved the BHE extraction rate. Another work ([31]) presented the exergy analysis of a hybrid GSHP system, coupled with solar panels, and indoor air conditioning was possible because of radiant panels with encapsulated PCM. The results showed that PCM was beneficial in term of first and second law efficiency; it increased with density and melting temperature.

The work presented in this paper follows the second approach. We propose the inclusion of an upstream (i.e., between the BHE and the HP) thermal energy storage in the standard GSHP layout. A similar approach is given in [32], where five different control methods for an air-to-air HP were implemented and coupled to a PCM-based TES to optimize its charge/discharge step with electricity tariffs and user demand. Solar-assisted GSHP were analyzed in [33], where the PCMs within the hot water puffer increased the amount of stored solar energy and generally improved the global COP. The importance of thermal storage in these hybrid systems was also confirmed by the experimental campaign in [34] and the numerical analysis in [35].

Finally, the works specifically focused on geothermal systems are [36,37], where PCM-based and sensible, respectively, downstream thermal storage (i.e., between the HP and the air distribution system) were coupled to a GSHP. On the one hand, in a comparison of the annual thermal energy use, at variable partial load ratio, of a boiler-based air conditioning system vs. conventional GSHP vs. TES-upgraded GSHP, the latter showed the best performance in terms of energy-savings. On the other hand, a similar configuration was seen for the cooling of an office building using different cooling storage ratios of PCM storage (i.e., the cooling capacity of PCM on the total building cooling capacity). The optimal cooling capacity was estimated to be 40%, which produced a decrease of 34% of the annual energy cost if compared to a GSHP system without TES.

In this work two different prototypal layouts were assessed and compared: a sensible-heat TES (SH-TES), where water was used as thermal storage material, and a latent-heat TES based on PCMs (PCM-TES). A first energy analysis using computational fluid dynamics of both scenarios was available in a previous work [38]. Based on these results, the work presented here is an in-depth evaluation of the respective energy performance and environmental impacts, measured and compared throughout whole life cycles, with the final aim of defining the most efficient and sustainable system configuration.

Section 2 gives a short description of the methodology. The case study is presented in Section 3. The results are shown in Section 4. Conclusions are discussed in Section 5. Extended results are given in the Supplementary Material.

2. Materials and Methods

All the potential environmental impacts of the proposed energy systems were quantified by the life cycle assessment (LCA) approach. This technique can be successfully used as a comparative analysis of different products or technologies providing the same service, in order to recognize the most efficient and environmentally sustainable option [39,40]. A life cycle assessment is a standardized and

widespread approach allowing the evaluation of environmental impacts associated with any process, product, or service throughout its entire life, usually starting from raw material acquisition until the end-of-life stage. Thanks to this approach, the life cycle of the studied product could be split into several parts corresponding to relevant components and/or phases (i.e., steps of the production and usage). The relative environmental weight of each part was explicitly assessed in order to spot and, possibly, optimize, the most impactful ones.

Our study, in accordance with standard LCA guidelines [41,42], was undertaken using the following steps:

1. Compilation of the life cycle inventory (LCI)—an input database based on product specifications (e.g., functional unit, system time and spatial boundaries, and quality criteria) that details all of the mass and energy flows, relative to each stage of the considered life cycle. The LCI is a collection of data, usually in a tabular form, used as input of the LCA model;
2. Quantification of the environmental impacts by relevant mid- and end-point indicators—the former evaluates the environmental burden as a function of single physical quantities. The latter takes into account higher aggregation levels, such as human health or biodiversity, for which information from multiple mid-point indicators is necessary. They are quantified by arbitrary units (Pt) instead of physical quantities. Mid-point indicators were taken from the comprehensive suite CML-IA baseline V3.05 [43]. End-point indicators were computed by the ReCiPe 20106 Endpoint (H) V1.03 method [44].

The aim of this work was to measure the environmental impact of two innovative GSHP layouts. The comparative approach was as follows: Starting from a reference layout used as a benchmark (i.e., baseline scenario), the enhancement of its energy performance and environmental impacts gained by the two proposed TES systems was measured in terms of mid- and end-point indicators. Different operative conditions were also evaluated for each system. All results were validated against experimental data measured using an existent prototype with a sensible-heat thermal storage and a small-scale laboratory unit with a latent-heat thermal storage.

The life cycle was modeled using the SimaPro v9.0.0 software [45] and the ecoinvent v3.5 database [46]. The impacts were computed according to the product category rule (PCR) document relative to electricity, steam and hot/cold water generation and distribution version 3.1 [47]. In this study, the following environmental indicators were considered

1. Mid-point indicators:
 - global warming in equivalent kgCO_2 ;
 - photochemical oxidation in equivalent kgC_2H_4 ;
 - acidification in equivalent kgSO_2e ;
 - eutrophication in equivalent kgPO_4^{3-} .
2. End-point indicators:
 - human health;
 - ecosystems;
 - resources.

3. The Case-Study

The system under investigation is a conventional ground-source heat pump system, used air-condition commercial buildings, characterized by a peak power of 17 kW, a yearly demand of 19,965 kWh of heating energy, and 4918 kWh of cooling energy, for a total of 24,883 kWh/year provided by the heat pump [48]. The baseline configuration (BAS) of this system consists of:

- a 17-kW reversible ground-source heat pump;

- and a total of 3 double-loop boreholes, each one 120 m deep with an average extraction capacity of 46.5 W/m measured by the ground response test.

This setup was upgraded by including upstream thermal storage (uTES) between the borehole heat exchangers and the heat pump [49]. The uTES was sized based on the maximum daily energy need instead of the maximum power. This new layout was designed to exchange heat with the ground even when it was not needed by the building, and using the thermal storage as a peak-shaving component. While average power exchanged with the ground on the one side and with the heat pump on the other side was the same, the maximum power required by the ground was less than the maximum power required by the heat pump as the former works with a higher duty cycle. On-site monitoring of a real-building prototype [50] confirmed that this layout was able to successfully decouple the energy exchange between the ground and the HP, resulting in a substantial reduction of peak geothermal power and, therefore, reduced borehole size (i.e., shorter/fewer boreholes to be drilled). Figure 1 shows the upgraded layouts with respect to the BAS scenario. They both use the same 17 kW heat pump while using just 1 borehole in combination with an uTES properly configured for each setup as follows:

- The sensible heating thermal energy storage (SH-TES) scenario used a concrete made tank of 12 m³ and the thermal storage material was water;
- The PCM thermal storage (PCM-TES) scenario was obtained using a PCM-based component instead of water. The storage was made of two PCM stacks of 2057 kg (RT-6 PCM) and 1233 kg (RT-27 PCMs) for nominal latent heat of 80 kWh and 50 kWh, respectively, and a total storage volume of about 1 m³.

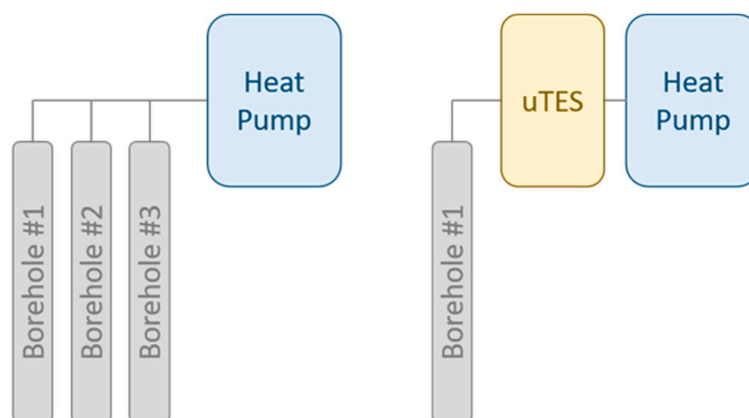


Figure 1. Layouts of the baseline setup (left) and the upgraded setup using an upstream thermal storage (uTES) (right).

As shown in a previous LCA study [48], the sensible-heat uTES was already able to reduce the environmental impact of the conventional layout. However, this preliminary analysis was limited to the evaluation of the environmental impact of the SH-uTES scenario, proposed first as an upgraded conventional BAS system. The inclusion of a latent-heat TES was already mentioned as a potential future development to reduce the storage volume, without any reference to its environmental issues. Similarly, the preliminary CFD energy analysis [38] detailed in the following paragraph exclusively calculated in terms of global COP, the performance of the PCM-uTES scenario. A more detailed assessment of the environmental impact of this system is presented in the current LCA analysis, where the environmental impacts of the PCM-TES system were measured during the life cycle of the plant (20 years), considering the energy consumption of a reference year. The obtained results were compared with a baseline scenario (BAS) and a sensible-heat thermal storage (SH-TES) scenario. For all three scenarios, two hypotheses were proposed: (a) electric energy is taken from the grid, and (b) electric energy is produced entirely from photovoltaic panels.

3.1. PCM Modeling and Validation

The energy performance of the PCM-TES scenario was already calculated by a comparative CFD analysis in [38], between the sensible and the latent uTES. Both systems abide by the same daily energy demand schedule, implemented on the basis of yearly energy consumption (see Section 3) and building characteristics [50]. The PCM-TES scenario simulated by CFD analysis provided two closed loops connected to the heat pump and the borehole, respectively. The heat transfer fluid within each loop entered a serpentine tube that crossed two different PCM stacks. The heat transfer between the borehole and PCM during the winter season was modeled via the following steps:

1. The heat transfer fluid (water) from the borehole flowed into the PCM storage;
2. This flow crosses the serpentine and, meanwhile, released heat into the PCMs in direct contact with tube shell;
3. Finally, it left the storage and entered the BHE again;
4. While the previous steps were running, the heat transfer fluid from the heat pump flowed to the PCM storage and withdrew the heat stored in latent form. The cycle was inverted in the summer season.

The results of this preliminary analysis clearly showed the twofold benefits of the PCM-TES scenario. On the one hand, the daily needs were fully covered by 10 times less thermal storage and, on the other hand, the reduction of storage temperature oscillations, as an effect of phase transition, increased the overall COP from 3.4, for both heating and cooling, to 4.13 and 5.89 for the heating and cooling modes, respectively.

An experimental campaign for the CFD model validation using data from a 1-kWh scale prototype is currently ongoing [51]. Figure 2 shows the experimental apparatus. It consists of two open loops connected to a boiler and a chiller, respectively. Each loop has its circulation pump. The PCM-storage connects both loops and collects the flows; these get mixed within the storage and exchange heat with the PCMs. (They present the same properties used in the CFD analysis.) The heating cycle took place in the following way:

1. The boiler that reproduced the BHE heated the water;
2. The heat was released to the PCM and stored in latent form;
3. The cooling water, produced by the chiller representing the heat pump, flowed within the storage and withdrew the stored heat.

Data were measured by two calorie flow meters placed at the outlet sections of the storage. The PCM phase transition was modeled as function of their temperature (T_{PCM}) and the thermo-physical properties (Table 1). When T_{PCM} achieved the melting/solidification point, the phase change started and the heat was stored in latent form along the transition region (± 0.25 °C with respect to the nominal transition temperature). Preliminary experimental data collected from the laboratory unit are shown in Figure 3. Good agreement between the simulated and measured outlet temperature (T_{out}) was observed using nominal PCM properties before any model calibration, strengthening the above estimates on performance improvement. CFD simulations were performed using a constant power equal to the average power measured during the experimental campaign. More detailed analyses will be presented in future works.

Table 1. PCM thermal properties.

PCM	Melting Range (°C)	Heat of Fusion (kJ/kg)	Sensible Heat (kJ/kg)		Density (kg/m ³)	
			Solid	Liquid	Solid	Liquid
RT6	8.0–8.5	140	1.8	2.4	860	770
RT27	25.0–25.5	146	1.8	2.4	870	750

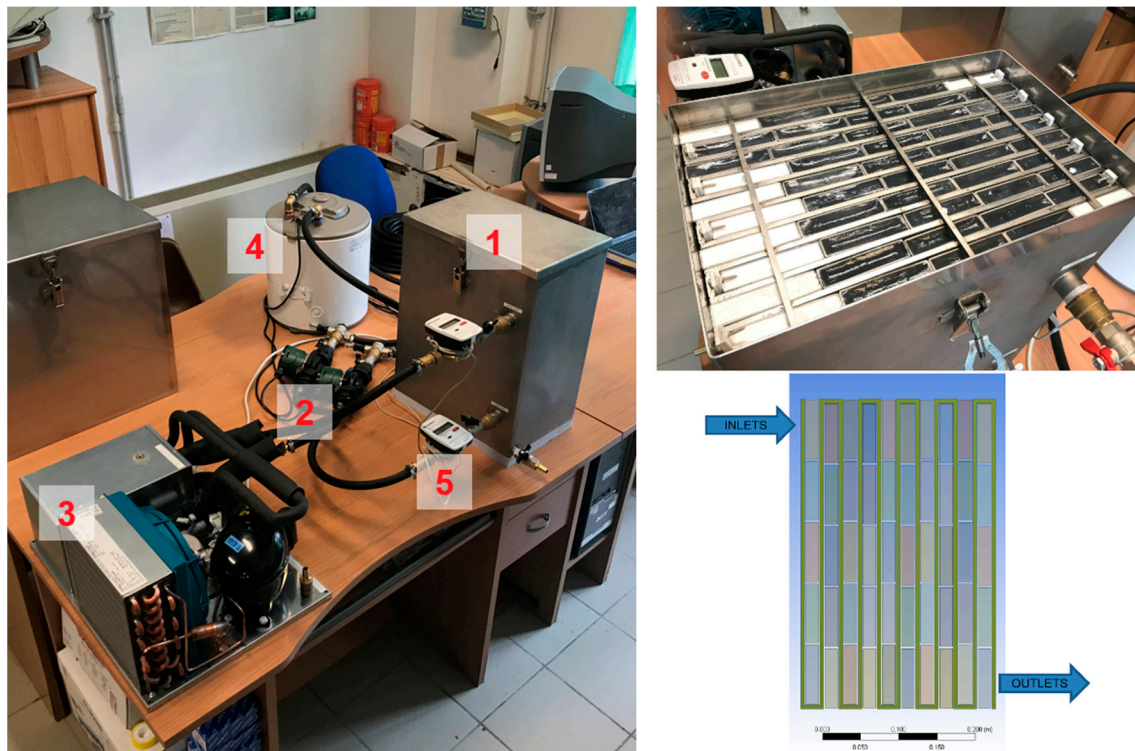


Figure 2. (left) Overview of the experimental layout. 1: phase-change-material (PCM) thermal storage, 2: circulating pumps, 3: chiller, 4: heater, 5: temperature/flow meters. (right) Close view of the PCM storage and top view of its geometry model.

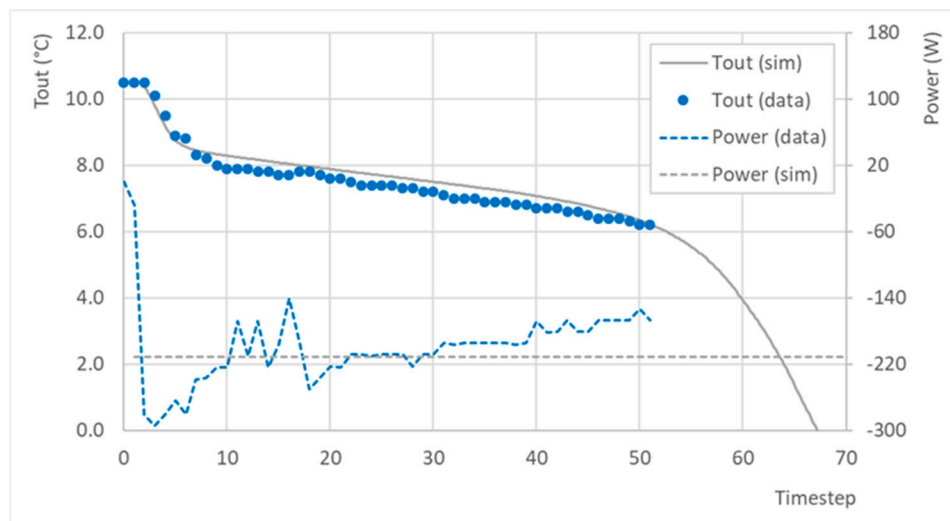


Figure 3. RT-6 PCM transition region: simulated vs. experimental data.

3.2. The Life Cycle Inventory

The three scenarios differ by borehole number, storage type, and electric energy consumption for heat production (the incidence of raw materials is reported in Table 2); the final electric energy consumption of each scenario is given by the respective COP values (Table 3). These values can be considered a conservative estimate as no contribution from cooling (heating) material is considered for the size of the heating (cooling) material (i.e., the effect of sensible heat of the cooling-optimized PCM is not considered on heating and vice versa).

Table 2. Material inventory of each scenario.

Scenario	BAS		SH-TES			PCM-TES		
Material/Process	Boreholes	Heat Pump	Boreholes	SH-uTES	Heat Pump	Boreholes	PCM-uTES	Heat Pump
Polyethylene (kg)	428	-	140	7.57	-	140	7.57	-
Sand (kg)	40,526	-	10,120	10.189	-	10,120	-	-
Gravel (kg)	53,606	-	13,398	13,440	-	13,398	-	-
Excavation (m ³)	55.9	-	14.0	76.4	-	14	-	-
Water (kg)	583	-	191	17,510	-	191	3510	-
Glycol (kg)	258	-	84.4	4.56	-	84.4	4.56	-
Concrete (m ³)	3.63	-	1.21	1.58	-	1.21	1299	81.0
Steel (kg)	105	81.0	43.0	428	81.0	43.0	-	-
Brass (kg)	-	6.00	-	8.00	-	-	8.00	-
Insulation (kg)	-	21.8	-	-	27.80	-	23.9	27.8
PCM (kg)	-	-	-	-	-	-	3290	-
Heat Pump (kW)	-	17.0	-	-	17.00	-	-	17.0
Al tape (m ²)	-	10.0	-	-	10.00	-	-	10.0

Table 3. Coefficient of performance (COP) and yearly electricity consumption of each scenario.

Scenario	COP		Electric Energy (kWh/year)	
	Heating	Cooling	Heating	Cooling
BAS	3.50	4.00	5704	1230
SH-TES	3.39	3.41	5889	1442
PCM-TES	4.13	5.89	4834	835

3.3. Functional Unit and System Boundaries

The functional unit in this study was 1 kWh of thermal energy (kWht) provided by the heat pump to the thermal energy distribution system. The impacts associated with the functional unit were obtained considering the energy inputs during the reference year and allocating the results based on the total production of heating and cooling energy. The system boundaries included the production of input materials for the implementation of the system from the boreholes to the heat pump, excavation activities for the boreholes and the sensible-heat storage, electric energy consumption, and end-of-life of the thermal storage and heat pump.

4. Results

4.1. Mid-Point Indicators

Results for mid-point indicators are shown in Tables 4 and 5, considering electric energy from the grid and from photovoltaic panels, respectively. The percentage variation was relative to the corresponding baseline scenario. We observed that, in terms of overall GHG emissions, the PCM-TES scenario was the most systematically competitive thanks to its higher overall COP that reduced primary energy consumption. This particularly impacted the case where electric energy was taken from the grid (−16% and −17% with respect to BAS and SH-TES scenarios, respectively). It can be noted that the SH-TES scenario had slightly higher impact as a direct consequence of COP deterioration (see Table 3). If electric energy was produced entirely by photovoltaic panels, the average reduction in impact indicators for the PCM-TES scenario would be approximately 69% (76% for CO₂e). Even in the PV hypothesis, the PCM-TES scenario performed best (−11% and −3.5% with respect to BAS and SH-TES scenarios, respectively). In all cases, the most impactful process was the consumption of electric energy. For the baseline scenarios, it accounted for an average of 85% using the grid hypothesis (Table 6) and 64% using the PV hypothesis (Table 7). Such values dropped to 64% and 41% for the PCM-TES scenarios, respectively. This result was produced by the fact that emission factors for PV production (multi-Si, 3 kWp) were, on average, 75% lower than emission factors for grid electricity (Italy, low voltage).

Table 4. Mid-point indicators for the three scenarios (electricity from grid).

Indicator	Units	Scenario				
		BAS, Grid	SH-TES, Grid		PCM-TES, Grid	
Global warming	kgCO ₂ e/kWh	0.130	0.132	+1.6%	0.108	−16.6%
Photochemical oxidation	gC ₂ H ₄ e/kWh	0.0307	0.0305	−0.8%	0.0246	−19.9%
Acidification	gSO ₂ e/kWh	0.728	0.743	+2.0%	0.620	−14.8%
Eutrophication	gPO ₄ ^{3−} e/kWh	0.237	0.239	+1.2%	0.209	−11.8%
Average variation (with respect to BAS)				+1.0%		−15.8%

Table 5. Mid-point indicators for the three scenarios (electricity from photovoltaic sources).

Indicator	Units	Scenario				
		BAS, PV	SH-TES, PV		PCM-TES, PV	
Global warming	kgCO ₂ e/kWh	0.0356	0.0323	−9.3%	0.0312	−12.2%
Photochemical oxidation	gC ₂ H ₄ e/kWh	0.0122	0.0109	−10.8%	0.00948	−22.5%
Acidification	gSO ₂ e/kWh	0.209	0.194	−7.2%	0.195	−6.4%
Eutrophication	gPO ₄ ^{3−} e/kWh	0.110	0.105	−4.1%	0.105	−4.4%
Average variation (with respect to BAS)				−7.8%		−11.4%

Table 6. Incidence of highest impact processes (electricity from grid).

BAS, Grid				
Process	Global Warming	Photochemical Oxidation	Acidification	Eutrophication
Electricity, grid	87.85%	82.45%	88.32%	82.85%
Heat pump	4.12%	5.80%	4.88%	9.84%
Propylene glycol	1.86%	3.79%	1.39%	2.43%
Gravel	1.50%	2.06%	1.58%	1.37%
Polyethylene	1.38%	1.81%	0.83%	0.24%
Concrete	1.26%	0.69%	0.64%	0.56%
SH_TES, Grid				
Process	Global Warming	Photochemical Oxidation	Acidification	Eutrophication
Electricity, grid	91.41%	87.92%	91.52%	86.57%
Heat pump	4.05%	5.85%	4.78%	9.72%
Propylene glycol	0.63%	1.32%	0.47%	0.83%
Gravel	0.74%	1.04%	0.78%	0.68%
PCM-TES, Grid				
Process	Global Warming	Photochemical Oxidation	Acidification	Eutrophication
Electricity, grid	86.10%	84.18%	84.79%	76.83%
Heat pump	4.94%	7.24%	5.73%	11.16%
Paraffin	4.56%	5.33%	5.57%	3.16%
Steel, low-alloyed	4.36%	8.91%	3.14%	7.22%
Steel and iron (waste treatment)	−4.11%	−12.07%	−2.93%	−2.65%

Table 7. Incidence of highest impact processes (electricity from photovoltaic).

BAS, PV				
Process	Global Warming	Photochemical Oxidation	Acidification	Eutrophication
Electricity, PV	55.65%	55.88%	59.24%	63.01%
Heat pump	15.03%	14.58%	17.02%	21.22%
Propylene glycol	6.78%	9.54%	4.85%	5.23%
Gravel	5.46%	5.18%	5.52%	2.95%
Polyethylene	5.05%	4.55%	2.90%	0.53%
Concrete	4.60%	1.73%	2.24%	1.20%
SH_TES, PV				
Process	Global Warming	Photochemical Oxidation	Acidification	Eutrophication
Electricity, PV	64.89%	66.24%	67.47%	69.45%
Heat pump	16.57%	16.34%	18.34%	22.12%
Propylene glycol	2.58%	3.69%	1.80%	1.88%
Gravel	3.02%	2.91%	2.98%	1.54%
Concrete	3.90%	1.49%	1.85%	0.96%
PCM-TES, PV				
Process	Global Warming	Photochemical Oxidation	Acidification	Eutrophication
Electricity, PV	51.82%	58.93%	51.72%	53.91%
Heat pump	17.11%	18.81%	18.18%	22.20%
Paraffin	15.82%	13.83%	17.67%	6.29%
Steel, low-alloyed	15.13%	23.13%	9.97%	14.36%
Propylene glycol	2.66%	4.24%	1.78%	1.89%
Steel and iron (waste treatment)	−14.25%	−31.33%	−9.31%	−5.28%

Tables 6 and 7 clearly show that processes related to the PCM-uTES introduced non-negligible impacts. From a life cycle perspective, it is, therefore, worth investigating if possible optimization of such processes might be viable and rewarding. Paraffins and steel, with similar shares, account for approximately 9% using the grid hypothesis, and 31% using the PV hypothesis. Considering these values, an optimal scenario might be foreseen (as discussed in Section 4.2) including the selection of bio-based PCMs and the minimization of steel in the storage structure with respect to the non-optimized prototypal layout.

4.2. Global Warming

The system life cycle was divided into six parts according to physical and usage boundaries. In addition, a detailed analysis on the global warming indicator was performed using this partition. The tree view of the PCM-uTES scenario considering electricity from the grid is given in Figure 4. The LCA indicators were:

1. BOREHOLES—containing borehole materials (tubes, concrete, etc.) and excavation;
2. STORAGE—containing different inputs according to different scenarios, including all raw materials, manufacturing/building processes, and piping;
3. HEAT PUMP—containing the HP machine, piping and insulation;
4. HEATING—containing electric energy consumption for heating (grid/PV hypotheses);
5. COOLING—containing electric energy consumption for cooling (grid/PV hypotheses);
6. END-OF-LIFE—containing recycling processes for separable materials (e.g., steel) and specific disposal for the reminder.

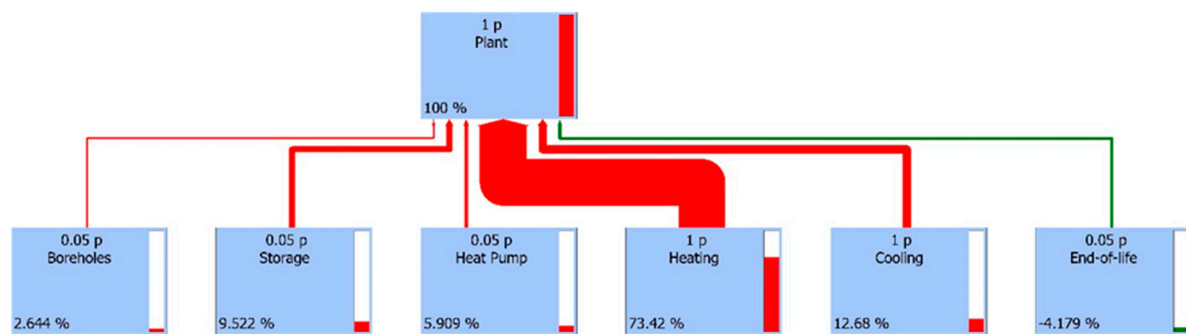


Figure 4. Typical tree view of the system life cycle (shown as global warming for the PCM-uTES scenario with energy from the grid).

The relative incidence of each part of the total GHG emissions is shown in Table 8. The phase-change material thermal energy storage was characterized by an impact higher than the water storage, mainly because of the steel and PCMs. However, a large part of its impact (44%) was compensated by the end-of-life indicator, during which steel can be recycled.

Table 8. Incidence of different life-cycle assessment (LCA) parts on global warming.

Part Scenario	Boreholes	Storage	Heat Pump	Heating	Cooling	End-of-life
BAS, grid	7.2%	0.0%	4.9%	72.3%	15.6%	0.0%
SH-TES, grid	2.2%	1.5%	4.8%	73.4%	18.0%	0.1%
PCM-TES, grid	2.6%	9.5%	5.9%	73.4%	12.7%	−4.2%
Part Scenario	Boreholes	Storage	Heat Pump	Heating	Cooling	End-of-life
BAS, PV	26.4%	0.0%	18.0%	45.8%	9.9%	0.0%
SH-TES, PV	8.9%	6.0%	19.8%	52.1%	12.8%	0.5%
PCM-TES, PV	9.2%	33.0%	20.5%	44.2%	7.6%	−14.5%

Details of the PCM-uTES are given in Table 9. PCMs and steel accounted for the highest impacts (42% and 40%, respectively). The amount of steel was computed using a direct proportion based on the 1-kWh lab prototype of storage. It was, therefore, straightforward to hypothesize lower incidence of steel for an optimized production-ready component. An optimal scenario was finally foreseen using bio-based PCMs and a reduced amount of steel. In the case of bio-based alternatives, the emission factor for PCMs could be lowered from 0.747 kgCO₂e/kg (ecoinvent, generic paraffin) down to 0.278 kgCO₂e/kg [52]. Considering the optimization of the PCM storage design, a reduction of 0.5 mm in the wall and tube thickness could be hypothesized for the production step without compromising the structure strength, resulting in a savings of approximately 40% of raw materials with respect to the non-optimized prototype design.

Table 9. Details of the PCM-uTES.

Process	Global Warming		Photochemical Oxidation		Acidification		Eutrophication	
	kgCO ₂ e	%	gC ₂ H ₄ e	%	gSO ₂ e	%	gPO ₄ ^{3−} e	%
Polyethylene	15.7	0.31%	4.87	0.26%	53.1	0.18%	5.05	0.04%
Water	1.98	0.04%	0.50	0.03%	9.10	0.03%	4.18	0.03%
Propylene glycol	21.2	0.41%	10.3	0.55%	89.0	0.30%	50.5	0.41%
Brass	50.5	0.99%	81.0	4.32%	2028	6.89%	1314	10.7%
Paraffin (RT-6)	1537	30.0%	408	21.7%	10,743	36.5%	2051	16.8%
Paraffin (RT-27)	921	18.0%	244	13.0%	6440	21.9%	1230	10.1%
Steel	2351	45.8%	1091	58.2%	9690	32.9%	7494	61.3%
Polystyrene	231	4.50%	34.9	1.86%	386	1.31%	85.2	0.70%
Total	5130	100%	1875	100%	29,439	100%	12,233	100%

The optimal scenario (PCM-TESopt, PV), realized using the above criteria and tested using the PV hypothesis, resulted in a 51% decrease in the global warming impact associated with the PCM-uTES, and an additional reduction of 10% with respect to the PCM-TES, PV scenario. The overall emission factor for the optimal scenario would be 0.028 kgCO₂e/kWh, −78% and −21% with respect to BAS, grid and BAS, PV scenarios, respectively.

4.3. End-Point Indicators

The results of the end-point indicators are shown in Figure 5. Impacts on human health are responsible for 93% of average overall impacts. As part of the electricity-from-grid hypothesis, the PCM-TES scenario showed a decrease of 10% with respect to the baseline. On the other hand, an increase of 1.3% was observed using the photovoltaic hypothesis. In this case the PCM-uTES introduced a positive impact (+25.6%) that was slightly higher than the overall reduction due to shorter boreholes (−13.5%) and lower energy demand for heating (−7.4%) and cooling (−3.3%).

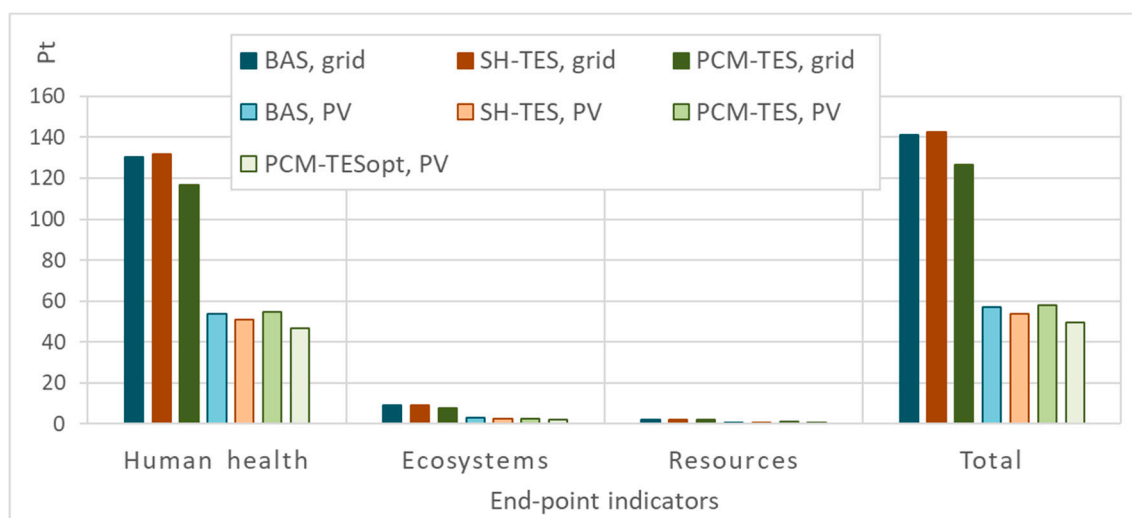


Figure 5. End-point indicator results.

The optimal scenario would likely lower the impacts of storage, resulting in the overall best performing layout, also in terms of end-point indicators (−64% and −13% with respect to BAS, grid and BAS, PV, respectively).

5. Conclusions

The LCA analysis was applied to a customized ground-source heat pump system. The innovative layout featured upstream thermal energy storage that was able to decouple the thermal fluxes from/to the ground and from/to the heat pump. Following the results of the experimental campaign, an upgrade TES component was evaluated using phase change materials instead of water. We showed that PCMs could reduce the volume of storage by a factor of 10 and enhance the system COP because of temperature stabilization during the charge/discharge cycles. The environmental performance of the system was evaluated in terms of mid- and end-point indicators per unit of thermal energy provided to the building considering the following two hypotheses: (1) energy is taken from the grid, and (2) energy is supplied by photovoltaic panels.

We found that the exploitation of phase-change materials allowed for sensible reduction of electric energy consumption (−18%) thanks to an improved COP both in terms of heating (from 3.50 to 4.13) and cooling mode (from 4.00 to 5.89). This resulted in an overall variation of mid-point indicators of −16% and −11% with respect to hypotheses (1) and (2), respectively. End-point indicator variation was −10% and +1.3%, respectively. The increase in the end-point indicators with respect to the PV hypothesis was due to the high relative impact of the PCM storage itself. Considering further, realistic,

optimization of the prototypal storage design using the PV hypothesis, mid- and end-point impacts could be as low as −78% and −64%, respectively, with respect to the baseline scenario (grid hypothesis), making it the most sustainable option.

In terms of global warming, the baseline scenario was characterized by 1.30 kgCO₂e/kWh (grid) and 0.0356 kgCO₂e/kWh (PV). The grid-hypothesis result was consistent with a previous study (0.156 kgCO₂e/kWh [50]), the difference being the higher value of the emission factor of electricity in the database used (ecoinvent v 3.2 [53]). The proposed PCM-TES layout could lower impacts by as much as 0.108 kgCO₂e/kWh and 0.0312 kgCO₂e/kWh for the grid and PV hypothesis, respectively. This would make such a solution very attractive to sensibly reduce both energy consumption (−21%) and the environmental impacts associated with space conditioning.

Supplementary Materials: The following are available online at <http://www.mdpi.com/1996-1073/13/1/117/s1>, Table S1: Mid-point indicators (CML-IA baseline V3.05) for the three scenarios (electricity from grid), Table S2: Mid-point indicators (CML-IA baseline V3.05) for the three scenarios (electricity from PV), Table S3: Incidence of most-impacting processes (BAS, grid), Table S4: Incidence of most-impacting processes (SH-TES, grid), Table S5: Incidence of most-impacting processes (PCM-TES, grid), Table S6: Incidence of most-impacting processes (BAS, PV), Table S7: Incidence of most-impacting processes (SH-TES, PV), Table S8: Incidence of most-impacting processes (PCM-TES, PV).

Author Contributions: Conceptualization, E.B. and A.A.; methodology, E.B.; software, E.B.; data curation, E.B. and A.A.; writing—original draft preparation, E.B.; writing—review and editing, E.B. and A.A.; supervision, E.B.; project administration, E.B.; funding acquisition, E.B. All authors have read and agreed to the published version of the manuscript.

Funding: This research was funded by Fondazione Cassa di Risparmio di Perugia, grant number 2017.0237.021.

Conflicts of Interest: The authors declare no conflict of interest.

References

1. European Commission. *A Roadmap for Moving to a Competitive Low Carbon Economy in 2050*; European Commission: Brussels, Belgium, 2011.
2. European Commission. *Horizon 2020 Work Programme for Secure, Clean, and efficient Energy*; European Commission: Brussels, Belgium, 2019.
3. Schwarz, M.; Nakhle, C.; Knoeri, C. Innovative designs of building energy codes for building decarbonization and their implementation challenges. *J. Clean. Prod.* **2019**, 119260. [\[CrossRef\]](#)
4. Intergovernmental Panel on Climate Change. *Global Warming of 1.5 °C—Chapter 2: Mitigation Pathways Compatible with 1.5 °C in the Context of Sustainable Development*; Intergovernmental Panel on Climate Change: Geneva, Switzerland, 2018.
5. Atanasiu, B.; Despret, C.; Economidou, M.; Maio, J.; Nolte, I.; Rapf, O.; Laustsen, J.; Ruyssevelt, P.; Staniaszek, D.; Strong, D.; et al. *Europe's Buildings under the Microscope: A Country-by-Country Review of the Energy Performance of Buildings*; Buildings Performance Institute Europe: Brussels, Belgium, 2011.
6. Cabeza, L.F.; Rincón, L.; Vilarinho, V.; Pérez, G.; Castell, A. Life cycle assessment (LCA) and life cycle energy analysis (LCEA) of buildings and the building sector: A review. *Renew. Sustain. Energy Rev.* **2014**, 29, 394–416. [\[CrossRef\]](#)
7. Cappello, M. *Efficienza Energetica Degli Edifici*; Grafill Editoria Tecnica: Palermo, Italy, 2008.
8. Bonamente, E.; Pelliccia, L.; Merico, M.; Rinaldi, S.; Petrozzi, A. The multifunctional environmental energy tower: Carbon footprint and land use analysis of an integrated renewable Energy plant. *Sustainability* **2015**, 7, 13564–13584. [\[CrossRef\]](#)
9. Bonamente, E.; Cotana, F. Carbon and energy footprints of prefabricated industrial buildings: A systematic life cycle assessment analysis. *Energies* **2015**, 8, 12685–12701. [\[CrossRef\]](#)
10. Wang, Z.; Zhao, J.; Li, M. Analysis and optimization of carbon trading mechanism for renewable energy application in buildings. *Renew. Sustain. Energy Rev.* **2017**, 73, 435–451. [\[CrossRef\]](#)
11. Vares, S.; Häkkinen, T.; Ketomäki, J.; Shemeikka, J.; Jung, N. Impact of renewable energy technologies on the embodied and operational GHG emissions of a nearly zero energy building. *J. Build. Eng.* **2019**, 22, 439–450. [\[CrossRef\]](#)

12. Asaleye, D.A.; Breen, M.; Murphy, M.D. A decision support tool for building integrated renewable energy microgrids connected to a smart grid. *Energies* **2017**, *10*, 1765. [[CrossRef](#)]
13. Sartori, I.; Hestnes, A.G. Energy use in the life cycle of conventional and low-energy buildings: A review article. *Energy Build.* **2007**, *39*, 249–257. [[CrossRef](#)]
14. Self, S.J.; Reddy, B.V.; Rosen, M.A. Geothermal heat pump systems: Status review and comparison with other heating options. *Appl. Energy* **2013**, *101*, 341–348. [[CrossRef](#)]
15. Curtis, R.; Lund, J.; Sanner, B.; Rybach, L.; Hellström, G. Ground source heat pumps—geothermal energy for anyone, anywhere: Current worldwide activity. *Proc. World Geotherm. Congr.* **2005**, *1437*, 1–9.
16. Ghasemi-Fare, O.; Basu, P. Predictive assessment of heat exchange performance of geothermal piles. *Renew. Energy* **2016**, *86*, 1178–1196. [[CrossRef](#)]
17. EU. Directive 2009/28/EC of the European Parliament and of the Council of 23 April 2009 on the promotion of the use of energy from renewable sources. *Off. J. Eur. Union* **2009**, *5*, 2009.
18. Braungardt, S.; Bürger, V.; Zieger, J.; Bosselaar, L. How to include cooling in the EU Renewable Energy Directive? Strategies and policy implications. *Energy Policy* **2019**, *129*, 260–267. [[CrossRef](#)]
19. Bu, X.; Ma, W.; Li, H. Geothermal energy production utilizing abandoned oil and gas wells. *Renew. Energy* **2012**, *41*, 80–85. [[CrossRef](#)]
20. Heier, J.; Bales, C.; Martin, V. Combining thermal energy storage with buildings—A review. *Renew. Sustain. Energy Rev.* **2015**, *42*, 1305–1325. [[CrossRef](#)]
21. Dincer, I. On thermal energy storage systems and applications in buildings. *Energy Build.* **2002**, *34*, 377–388. [[CrossRef](#)]
22. Cabeza, L.F.; Castell, A.; Barreneche, C.D.; De Gracia, A.; Fernández, A. Materials used as PCM in thermal energy storage in buildings: A review. *Renew. Sustain. Energy Rev.* **2011**, *15*, 1675–1695. [[CrossRef](#)]
23. Kenisarin, M.; Mahkamov, K. Passive thermal control in residential buildings using phase change materials. *Renew. Sustain. Energy Rev.* **2016**, *55*, 371–398. [[CrossRef](#)]
24. Cui, Y.; Zhu, J.; Twaha, S.; Chu, J.; Bai, H.; Huang, K.; Chen, X.; Zoras, S.; Soleimani, Z. Techno-economic assessment of the horizontal geothermal heat pump systems: A comprehensive review. *Energy Convers. Manag.* **2019**, *191*, 208–236. [[CrossRef](#)]
25. Piga, B.; Casasso, A.; Pace, F.; Godio, A.; Sethi, R. Thermal impact assessment of groundwater heat pumps (GWHPs): Rigorous vs. simplified models. *Energies* **2017**, *10*, 1385. [[CrossRef](#)]
26. Cui, P.; Yang, H.; Fang, Z. Numerical analysis and experimental validation of heat transfer in ground heat exchangers in alternative operation modes. *Energy Build.* **2008**, *40*, 1060–1066. [[CrossRef](#)]
27. Balbay, A.; Esen, M. Experimental investigation of using ground source heat pump system for snow melting on pavements and bridge decks. *Sci. Res. Essays* **2010**, *5*, 3955–3966.
28. Wang, G.; Wang, W.; Luo, J.; Zhang, Y. Assessment of three types of shallow geothermal resources and ground-source heat-pump applications in provincial capitals in the Yangtze River Basin, China. *Renew. Sustain. Energy Rev.* **2019**, *111*, 392–421. [[CrossRef](#)]
29. Zhang, S.; Zhang, L.; Wei, H.; Jing, J.; Zhou, X.; Zhang, X. Field testing and performance analyses of ground source heat pump systems for residential applications in Hot Summer and Cold Winter area in China. *Energy Build.* **2016**, *133*, 615–627. [[CrossRef](#)]
30. Yang, W.; Xu, R.; Yang, B.; Yang, J. Experimental and numerical investigations on the thermal performance of a borehole ground heat exchanger with PCM backfill. *Energy* **2019**, *174*, 216–235. [[CrossRef](#)]
31. Oruc, O.; Dincer, I.; Javani, N. Application of a ground source heat pump system with PCM-embedded radiant wall heating for buildings. *Int. J. Energy Res.* **2019**, *43*, 6542–6550. [[CrossRef](#)]
32. Jung, W.; Kim, D.; Kang, B.; Chang, Y. Investigation of heat pump operation strategies with thermal storage in heating conditions. *Energies* **2017**, *10*, 2020. [[CrossRef](#)]
33. Han, Z.; Zheng, M.; Kong, F.; Wang, F.; Li, Z.; Bai, T. Numerical simulation of solar assisted ground-source heat pump heating system with latent heat energy storage in severely cold area. *Appl. Therm. Eng.* **2008**, *28*, 1427–1436. [[CrossRef](#)]
34. Kaygusuz, K. Investigation of a combined solar-heat pump system for residential heating. Part 1: Experimental results. *Int. J. Energy Res.* **1999**, *23*, 1213–1223. [[CrossRef](#)]
35. Kaygusuz, K. Investigation of a combined solar-heat pump system for residential heating. Part 2: Simulation results. *Int. J. Energy Res* **1999**, *23*, 1225–1237. [[CrossRef](#)]

36. Seo, B.M.; Hong, S.H.; Choi, J.M.; Lee, K.H. Part load ratio characteristics and energy saving performance of standing column well geothermal heat pump system assisted with storage tank in an apartment. *Energy* **2019**, *174*, 1060–1078.
37. Zhu, N.; Hu, P.; Lei, Y.; Jiang, Z.; Lei, F. Numerical study on ground source heat pump integrated with phase change material cooling storage system in office building. *Appl. Therm. Eng.* **2015**, *87*, 615–623. [\[CrossRef\]](#)
38. Bonamente, E.; Aquino, A.; Cotana, F. A PCM Thermal Storage for Ground-source Heat Pumps: Simulating the System Performance via CFD Approach. *Energy Procedia* **2016**, *101*, 1079–1086. [\[CrossRef\]](#)
39. Vollaro, R.D.L.; Calvesi, M.; Battista, G.; Evangelisti, L.; Botta, F. Calculation model for optimization design of low impact energy systems for buildings. *Energy Procedia* **2014**, *48*, 1459–1467. [\[CrossRef\]](#)
40. Finnveden, G.; Hauschild, M.Z.; Ekvall, T.; Guinée, J.; Heijungs, R.; Hellweg, S.; Koehler, A.; Pennington, D.; Suh, S. Recent developments in life cycle assessment. *J. Environ. Manag.* **2009**, *91*, 1–21. [\[CrossRef\]](#)
41. International Organization for Standardization. *ISO 14044: Environmental Management, Life Cycle Assessment, Requirements and Guidelines*; International Organization for Standardization: Geneva, Switzerland, 2006.
42. International Organization for Standardization. *Environmental Management: Life Cycle Assessment; Principles and Framework*; Number 2006; International Organization for Standardization: Geneva, Switzerland, 2006.
43. CML-IA Characterization Factors. Available online: <https://www.universiteitleiden.nl/en/research/research-output/science/cml-ia-characterisation-factors> (accessed on 13 November 2019).
44. Goedkoop, M.; Heijungs, R.; Huijbregts, M.; De Schryver, A.; Struijs, J.; van Zelm, R. *ReCiPe 2008. A Life Cycle Impact Assessment Method Which Comprises Harmonised Category Indicators at the Midpoint and the Endpoint Level*; The Ministry of Housing, Spatial Planning and the Environment: Hague, The Netherlands, 2018.
45. SimaPro 9.0. Available online: <https://simapro.com/2019/whats-new-in-simapro-9-0/> (accessed on 13 November 2019).
46. Ecoinvent 3.5. Available online: <https://www.ecoinvent.org/database/older-versions/ecoinvent-35/ecoinvent-35.html> (accessed on 13 November 2019).
47. The International EPD System. *Product Category Rules: Electricity, Steam and Hot/Cold Water Generation and Distribution*; The International EPD System: Stockholm, Sweden, 2015.
48. Bonamente, E.; Aquino, A. Life-Cycle Assessment of an Innovative Ground-Source Heat Pump System with Upstream Thermal Storage. *Energies* **2017**, *10*, 1854. [\[CrossRef\]](#)
49. Moretti, E.; Bonamente, E.; Buratti, C.; Cotana, F. Development of innovative heating and cooling systems using renewable energy sources for non-residential buildings. *Energies* **2013**, *6*, 5114–5129. [\[CrossRef\]](#)
50. Bonamente, E.; Moretti, E.; Buratti, C.; Cotana, F. Design and monitoring of an innovative geothermal system including an underground heat-storage tank. *Int. J. Green Energy* **2016**, *13*, 822–830. [\[CrossRef\]](#)
51. ESCC 2016. Available online: <http://esc.uth.gr/esc-2019/> (accessed on 13 November 2019).
52. Heidari, M.D.; Mathis, D.; Blanchet, P.; Amor, B. Streamlined Life Cycle Assessment of an Innovative Bio-Based Material in Construction: A Case Study of a Phase Change Material Panel. *Forests* **2019**, *10*, 160. [\[CrossRef\]](#)
53. Ecoinvent 3.2. Available online: <https://www.ecoinvent.org/support/documents-and-files/information-on-ecoinvent-3/information-on-ecoinvent-3.html#1980> (accessed on 13 November 2019).



© 2019 by the authors. Licensee MDPI, Basel, Switzerland. This article is an open access article distributed under the terms and conditions of the Creative Commons Attribution (CC BY) license (<http://creativecommons.org/licenses/by/4.0/>).